

Compositional 3D Human-Object Neural Animation

Zhi Hou, Baosheng Yu, Dacheng Tao

The University of Sydney

<https://zhihou7.github.io/CHONA>

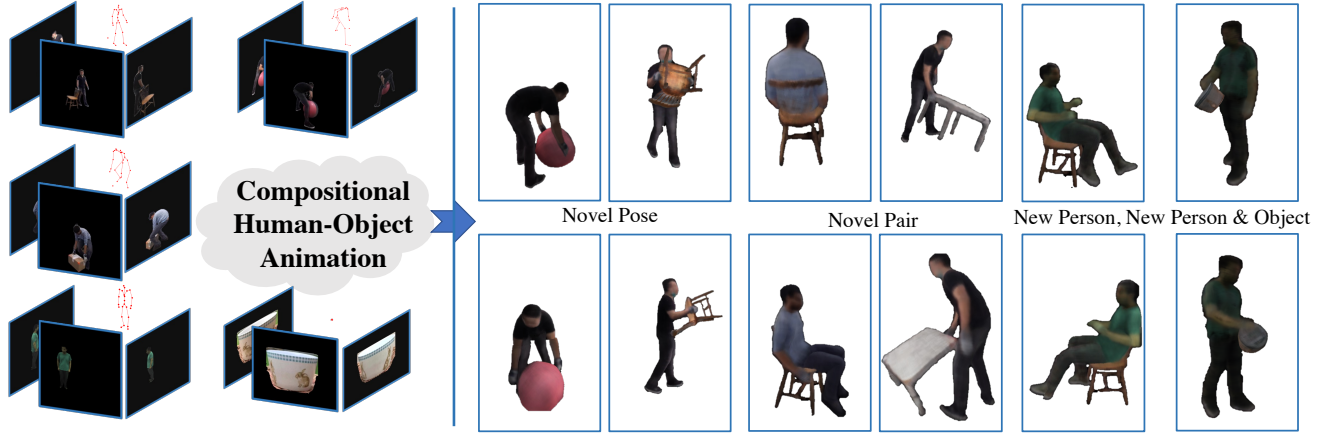


Figure 1: An illustration of compositional human-object neural animation. Given a set of sparse multi-view RGB HOI short videos with less than 50 frames, we render the neural animation of novel HOIs with novel pose, human, and object. Specifically, most faces in the training dataset are partly blurred.

Abstract

Human-object interactions (HOIs) are crucial for human-centric scene understanding applications such as human-centric visual generation, AR/VR, and robotics. Since existing methods mainly explore capturing HOIs, rendering HOI remains less investigated. In this paper, we address this challenge in HOI animation from a compositional perspective, i.e., animating novel HOIs including novel interaction, novel human and/or novel object driven by a novel pose sequence. Specifically, we adopt neural human-object deformation to model and render HOI dynamics based on implicit neural representations. To enable the interaction pose transferring among different persons and objects, we then devise a new compositional conditional neural radiance field (or CC-NeRF), which decomposes the interdependence between human and object using latent codes to enable compositionally animation control of novel HOIs. Experiments show that the proposed method can generalize well to various novel HOI animation settings. Code will be made publicly available.

1. Introduction

Rendering 3D human-object animation is of great importance for human-centric generation with a wide range of real-world applications such as telepresence, video games, films, content generation, AR/VR and robotics. However, reconstructing and rendering human avatars with the interactive objects remains poorly investigated. Since traditional 3D reconstruction methods highly depend on dense cameras or depth sensors [49, 10, 9], implicit neural representations for graphical objects present appealingly realistic results without the requirement of complex hardware and thus receive increasing attention from the community [35, 36, 3, 38, 67]. Specifically, [36] introduces an implicit representation, i.e., neural radiance fields (NeRF), which represents static or rigid 3D objects/scenes as color and density fields and is capable of efficiently learning 3D geometry from images with differentiable volume rendering techniques.

To explore dynamic non-rigid scenes and objects, vanilla NeRF has been recently extended to handle deforming scenes [42, 55, 45, 43] and motion modeling [29, 63, 46]. Though the deformation-based approaches [42, 43, 47]

achieve appealing results in handling dynamic scenes, they are usually limited to scenes with small variances (*e.g.*, faces). However, Human-centric interactions include large variances and extensive occlusions, which poses a significant challenge to directly model the dynamics with the interpolation methods [42, 43]. Recently, those neural linear skinning approaches represent multiple frames of human body with implicit neural representations under the control of skeleton [44, 32, 52, 27, 65, 39, 75, 28, 59], achieving considerable performance in free-viewpoint human avatar rendering and demonstrating good generalization to novel human poses [28, 59]. However, the above-mentioned methods usually focus on the animation of either individual human body or object, leaving the interactions between human and object poorly investigated. Particularly, the interactions are seriously self-occluded and it will hamper the modelling of human body. Meanwhile, several methods propose to explore the interactions between human and the surrounding objects or environments [54, 17, 13, 73, 8, 68, 66, 33]. Nevertheless, they mainly aim to reconstruct human/object shape and appearance rather than rendering animatable HOIs.

To jointly capture dynamic human body and objects with mutually occlusions, we thus generalize deformable neural radiance fields for human-object interaction with an additional point to indicate the objects. With a simple object modeling strategy, we can relieve the dependence on the object prior model (*e.g.* object meshes) and effectively improve the reconstruction of human and object under complex occlusions. Specifically, the objects are regarded as disconnected joints in correspondence to the human body, and we then construct “pseudo bones” based on the object joint together with human body bones to model and control the dynamics of human-object interactions. By doing this, we extend the idea of animatable volumetric avatars to human-object interactions with non-linear pose-dependent deformation fields. Therefore, with the carefully designed canonical human-object pose, the generalized deformation fields and coordinate-based volumetric rendering, we can reconstruct and animate existing self-occluded HOIs. Particularly, we notice those Mesh or SDF-based methods [44, 59] usually fail to reconstruct the complex object without object prior model (Please refer to Section 5.1). Considering that mesh or prior model is not always available for novel objects, we thus adopt 3D human pose and 6-DoF object pose to guide the reconstruction and rendering from multi-view images, and simplify the control of HOI animation. We introduce the details of neural human-object deformation in Section 3.3.

Nevertheless, it is impractical to obtain all those interaction poses for the rare objects, which will limit the application of Neural Human-Object Animation in the real world. Considering people usually interact with similar ob-

jects in the same way, we thus introduce a compositional human-object animation challenge, which is not only related to novel poses/actions but also novel human and object. To enable the compositionally animate human-object interaction, we introduce compositional conditional neural radiance fields (CC-NeRF) with latent codes for human and object respectively. Specifically, to facilitate the transfer of the interactions among different humans/objects, we then decompose the human and object latent codes via the compositional invariant learning. By doing this, we thus enable the controllable animation for novel human-object interactions. We introduce the details of compositional animation in Section 3.4.

In this paper, we present a novel approach, named as compositional 3D human-object neural animation or CHONA, to implicitly reconstruct HOIs from sparse multi-view videos via coordinate-based neural representations, and compositionally animate HOIs under novel poses/interactions, novel person and novel object. An illustration of compositional HOI animation is shown in Figure 1. Our contributions can be summarized as:

- We introduce an HOI animation framework by exploring neural HOI deformations.
- We devise a compositional conditional NeRF for compositional HOI animation, which enables transferring interaction poses to novel human and object.
- We perform comprehensive experiments to demonstrate that the proposed method not only improves the animation performance but also the compositional generalization.

2. Related Work

2.1. Human-Object Interaction

The interaction with objects is common in the people’s daily life [22, 12]. Early work mainly investigate synthesizing human pose and object [22], human body reconstruction [11], object recognition [61], or human 3d pose estimation [1, 25, 6, 30] under the interaction with objects or environments. Recently, Human-Scene Synthesis [69, 71, 18, 74, 57, 16, 56] has attracted extensive interests from the community due to the potential applications in the content generation. Those methods usually depend on the prior human model (*e.g.*, SMPL) and only synthesize the human motion in the scenes, while compositional Human-Object neural animation aims to animate both human and object in a compositional manner. Recently, increasing approaches [4, 54, 53, 14, 23, 8, 66, 68, 21, 60, 64] focus on 3D Interactions between Human and its surrounding objects. Zhang [68] present to reconstruct the spatial arrangements of Human-Object Interaction. [66, 8] reconstruct the meshes of human-object interactions, while recent

work [23] introduces the neural representations to human-object interaction and significantly advances the novel view synthesis performance. Particularly, a real HOI dataset, BEHAVE [4], consisting of 8 subjects and diverse objects, is introduced with spare views of HD videos and the poses of human and object. We mainly conduct our experiments based on BEHAVE. Concurrent work [15, 60, 64, 21, 70, 64, 76] focus on reconstruction, 3D tracking or motion refinement, significantly ignoring interaction animations. Besides, though current compositional approaches on human-centric interactions have studied the recognition [24], detection [19], object affordance [20], 2D generation [37], and 3D human-scene synthesis [74], the compositional 3D animation remains unsolved.

2.2. Animatable Avatars

3D Avatars [34, 45, 59, 28, 5, 72] have been through a significant progress. Early work usually leverages SMPL [34] model to reconstruct or synthesize human body, however the body is usually naked. Recently, neural fields have dominated 3D shape representations and novel view synthesis. Peng *et al.* [45] present to implicitly reconstruct human body from spare videos with neural radiance fields with a carefully designed skinning deformation. Next, [44, 32, 27, 39, 52, 31, 75, 51] significantly facilitate the performance in novel view rendering for novel poses. More recently, [28, 59] demonstrate appealing avatar generation under out of distribution poses. Meanwhile, [31, 62] presents to reconstruct high-fidelity human avatars from the monocular RGB video observation. Specifically, [51, 28] requires only 3D skeletons and multiple multi-view frames to construct an animatable Avatar, while [59] requires a pre-trained body SDF model to control the animation. Considering the fewer requirements on body models (*e.g.*, SMPL) of pose-dependent animation, we follow [51, 28] to compositionally control the animation.

2.3. Neural 3D Representations

Neural representations [41, 35, 7] have revolutionized the 3d surface representation, and achieved continuous, high resolution outputs of arbitrary shape. Recently, NeRF [36] represents 3D points in the scene with density and color, and renders the scene with volumetric rendering techniques, achieving photorealistic novel rendering. Next, [3] extends NeRF to represent the scene at a continuously-valued scale with conical frustum. GRAF [50] represents the neural radiance conditioned on shape/appearance latent codes. GIRAFFE [38] further presents controllable image synthesis with Compositional Generative Neural Feature Fields. However, those approaches [50, 38] mainly learn the representations from static scenes, in which the objects are not frequently occluded. Differently, Compositional Human-Object animation requires to control the syn-

thesis from spare multi-view HOI videos, which includes massive occlusion for human body and objects. Meanwhile, [50, 38, 67] mainly control the image synthesis for the static 3D scenes with rigid objects via linear transformation, while our approach is able to deform the interaction in a non-linear way.

3. Method

In this section, we introduce the proposed compositional 3D human-object animation approach. Specifically, we first provide an overview of HOI animation and the popular neural radiance fields (NeRF). We then introduce the neural human-object deformation and the compositional conditional radiance fields in detail.

3.1. Overview

Given sparse multi-view inputs, including interaction videos, single person videos, and objects, Compositional 3D Human-Object Animation enables to not only render the interaction under novel interaction pose, but also animate the interaction between a novel person and novel objects. Specifically, we build a pseudo bone for the object, and then treat the pseudo bone equally with body bones. Next, following the popular body skinning deformation techniques [44, 75, 28, 59], we devise a neural Human-Object deformation method to construct animatable human-object interactions as illustrated in Figure 2. Moreover, in order to control the interaction animation with novel people or objects, we devise compositional conditional radiance fields with two conditional latent codes, representing human and object respectively, to control the human-object identity. Specifically, we devise a compositional invariant learning strategy to decompose the interdependence between human and object latent codes, and thus enable to compositionally control the animation for novel objects or people.

3.2. Preliminary: Neural Radiance Fields

NeRF [36] leads to significant progress in a wide range of 3D vision topics. It implicitly represents the geometry and appearance of the scene with a multi-layer perceptron neural network and volumetric rendering techniques. For a ray r and the viewing direction (θ, ϕ) , NeRF first queries the emitted color c and density σ at the 3D point $x = (x, y, z)$ in the ray r , then uses volumetric rendering to get the pixel color $C(r)$ via accumulating the view-dependent colors along the ray r as follow,

$$C(r) = \sum_i^N T_i(1 - \exp(\sigma_i \delta_i)) c_i, \quad (1)$$

where $T_i = \exp(-\sum_{j=1}^{i-1} \sigma_j \delta_j)$, δ_i indicates the distances between the sample points along the ray. Then, it

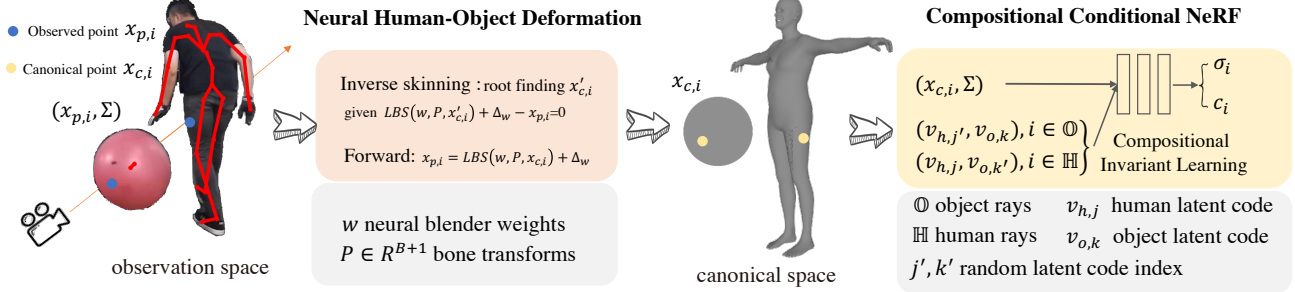


Figure 2: Overview of the proposed approach. The proposed compositional human-object neural animation approach leverages the neural Human-Object deformation module to deform the canonical points to posed points, and identify the corresponding canonical points of observed points via inverse skinning. Next, we obtain the density and color of the ray points conditioned on human and object latent codes, and accumulate the samples to render the pixel color. In addition, a compositional invariant learning strategy is introduced to decompose the interdependence between the two latent codes based on object and human masks, and facilitate compositional human-object animation.

optimizes the network via calculating the distance loss between $C(\mathbf{r})$ and ground truth pixel color. Recently, Mip-NeRF [3] extends NeRF via taking each point in the ray as a cone, the samples α along the ray as conical frusta modeled as multivariate Gaussians (μ, Σ) . Mip-NeRF accumulates the pixel color in a similar way to NeRF [36].

3.3. Neural Human-Object Deformation

To represent the human-object interaction via neural volumetric representation, we devise a neural Human-Object deformation as follows. For each point \mathbf{x}_p in the observed/posed space, we have a corresponding point \mathbf{x}_c in the canonical space, which can be deformed into \mathbf{x}_p via neural skinning deformation. The canonical representation includes a Lambertian neural radiance field $F_{\Theta_r} : (\mathbf{x}_c, \Sigma) \rightarrow (\mathbf{c}, \delta)$, where r denotes the pixel ray, $\mathbf{c} = (r, g, b)$ indicates the material color, δ represents the material density respectively. Besides, we follow Mip-NeRF [3] to accumulate the samples (\mathbf{x}_p, Σ) (a multivariate Gaussian) to render the pixel color at each ray. As illustrated in Figure 2, the canonical human-object space includes a T-pose body and an object placed in front of the body. We denote the transformation of each body bone as $\mathbf{T}_i, 0 \leq i < B$, where B is the number of body bones and $\mathbf{T}_i \in R^{4 \times 4}$. We represent the 6 DoF transformation (t, r) of the object from canonical space to the observed space as \mathbf{T}_B . As a result, we have $\mathbf{P} = \{\mathbf{T}_0, \mathbf{T}_1, \dots, \mathbf{T}_B\} \in R^{(B+1) \times 4 \times 4}$ representing the transformation of a human-object interaction.

Forward Skinning. Following the popular animatable avatar methods [5, 58, 59, 28], we revise the traditional linear blend skinning (LBS) [2, 34, 40] into neural skinning to deform a canonical Human-Object pose according to rigid bone transformations. We treat background as an

additional bone. Thus, we have $B + 2$ bones for the human-object interaction. Similar to [44, 59, 28], a MLP function $F_{\Theta_s} : \mathbf{x}_c \rightarrow \mathbf{w}$ is used to project a canonical point \mathbf{x}_c into corresponding weights \mathbf{w} . Given the skinning weights $\mathbf{w} = (w_0, w_1, \dots, w_{B-1}, w_B, w_{bg}) \in R^{B+2}$ and a pose $\mathbf{P} = \{\mathbf{T}_0, \mathbf{T}_1, \dots, \mathbf{T}_B\}$, we use forward LBS to define the deformation of a sample \mathbf{x}_c in the canonical space to \mathbf{x}_p in the view space:

$$\begin{aligned} \mathbf{x}_p &= LBS(F_{\Theta_s}(\mathbf{x}_c), \mathbf{P}, \mathbf{x}_c) + F_{\Theta_\nabla}(\mathbf{x}_c, \mathbf{P}) \\ &= \left[\sum_{j=0}^{B+1} F_{\Theta_s,j}(\mathbf{x}_c) \cdot \mathbf{T}_j + w_{bg} \cdot \mathbf{I} \right] \cdot \mathbf{x}_c + F_{\Theta_\Delta}(\mathbf{x}_c, \mathbf{P}), \end{aligned} \quad (2)$$

where $\mathbf{I} \in R^{4 \times 4}$ denotes identity matrix, $F_{\Theta_\Delta} : (\mathbf{x}_c, \mathbf{P}) \rightarrow \Delta_w \in R^3$ is for modeling the non-linear deformations [28].

Inverse Skinning. It requires to transform the observed points into canonical space for rendering the model. Similar to [5, 59, 28], we leverage the root finding strategy [5] to deform \mathbf{x}_p to \mathbf{x}'_c subject to,

$$f(\mathbf{x}'_c) = LBS(F_{\Theta_s}(\mathbf{x}'_c), \mathbf{P}, \mathbf{x}'_c) + F_{\Theta_\Delta}(\mathbf{x}'_c, \mathbf{P}) - \mathbf{x}_p = 0, \quad (3)$$

where \mathbf{x}'_c denotes the potential canonical point of \mathbf{x}_p . Then we solve it numerically via Newton's method similar to [59, 28], and we simply use the $K = 5$ nearest bones of the point in observed space to initialize the Newton's method for reducing the computational burden. We get K corresponding points $\{\mathbf{x}'_{c,0}, \mathbf{x}'_{c,1}, \dots, \mathbf{x}'_{c,K-1}\}$ for the observed point \mathbf{x}_p . With the canonical points, we follow [5, 28] to compute the gradients and render the image (See more details in Appendix).

3.4. Compositional Conditional Radiance Fields

Though the proposed human-object neural deformation enables the animation for a given human-object interaction, it fails to animate novel combinations, *i.e.* an interaction involves a novel person or a novel object. Due to the combinatorial explosion of Human-Object interactions and the challenges of capturing interaction poses, we can not collect the multi-view videos for all possible interactions, which significantly limits the potential applications of the proposed human-object neural deformation. Therefore, we devise Compositional Conditional Radiance Fields to enable compositionally animating the interactions from novel combinations, and even novel person and objects. To decouple the controlling of human and object, we use two latent codes for the Conditional Radiance Fields. Denote $\mathbf{v}_h \in R^{N_h \times C}$ and $\mathbf{v}_o \in R^{N_o \times C}$, where N_h and N_o are the numbers of person and object categories, as the latent codes of human and object respectively, we have the conditional radiance fields as follows,

$$F_{\Theta_r} : (\mathbf{x}_c, \Sigma, \mathbf{v}_{h,j}, \mathbf{v}_{o,k}) \rightarrow (\mathbf{c}, \boldsymbol{\delta}), \quad (4)$$

where $0 \leq j < N_h$ and $0 \leq k < N_o$ denote the corresponding person and object for observed interaction. With the conditional radiance fields, we can control the rendering for different human-object pairs with \mathbf{v}_h and \mathbf{v}_o . However, the two latent codes \mathbf{v}_h and \mathbf{v}_o are entangled together, *i.e.*, the rendering is controlled jointly by two latent codes. Therefore, the conditional radiance field in Eq. (4) fails to animate the interactions of novel human or objects.

Compositional Invariant Learning. To decouple the interdependence between the human and object latent codes, we further introduce a compositional invariant learning (CIL) strategy for conditional radiance fields, named as Compositional Conditional Radiance Fields, to ease the spurious correlation between human and object latent codes, and thus enable compositional neural animation. Specifically, for the pixel in human body, we expect $(\mathbf{c}, \boldsymbol{\delta})$ only dependent on \mathbf{v}_h , regardless of the value of \mathbf{v}_o . Thus, when the ray r is located in the human body, we randomly set the value for the object latent codes, and vice versa for rays in the object. Then, the color and density of the Compositional Conditional Radiance Fields for the points in ray r are presented as follows,

$$\mathbf{c}, \boldsymbol{\delta} = \begin{cases} F_{\Theta_r}(\mathbf{x}_c, \Sigma, \mathbf{v}_{h,j'}, \mathbf{v}_{o,k}) & r \in \mathbb{O} \\ F_{\Theta_r}(\mathbf{x}_c, \Sigma, \mathbf{v}_{h,j}, \mathbf{v}_{o,k'}) & r \in \mathbb{H} \end{cases} \quad (5)$$

where $\mathbb{H} \cap \mathbb{O} = \emptyset$, \mathbb{H} and \mathbb{O} represent the rays set of human and object respectively. j' and k' are random latent human and object codes respectively. Via randomly setting the latent codes, we can decouple the interdependence of

the Human-Object pairs in the training set. Therefore, we can control the animation via human or object latent codes individually.

4. Implementation Details

In this paper, we follow the linear blender skinning deformation [44, 59, 75, 28] to devise an additional pseudo bone for human-object interaction and two latent codes for compositional animation. We localize the human and object rays according to the provided segmentation in [4]. We model the shading effect similar to [28], and sample 64 points along a ray. Due to the camera distance difference between different datasets, we sample 2048 rays for BEHAVE images, 1024 rays for ZJU-mocap images, and 512 rays for CO3D images in each mini-batch. Meanwhile, we utilize two additional losses for skinning weights and non-linear deformations in [28] for optimization. The overall loss function thus is $\mathcal{L} = \mathcal{L}_{img} + \lambda \mathcal{L}_w + \beta \mathcal{L}_\Delta$, where \mathcal{L}_{img} indicates image loss similar to [36], \mathcal{L}_w represents the loss to encourage the onehot skinning weights w , \mathcal{L}_Δ is to encourage the non-linear deformation term $F_{\Theta_\Delta}(\mathbf{x}_c, \mathbf{P})$ close to zero. Both \mathcal{L}_w and \mathcal{L}_Δ are MSE losses. In our experiments, we set λ to 1.0 and β to 0.1. The Adam optimizer [26] is adopted for the training with an initial learning rate 5e-4 and an exponentially decay strategy to 5e-6.

5. Experiments

In this section, we perform experiments to quantitatively and qualitatively illustrate Human-object Animation, including novel poses, compositional animation, and even novel non-interactive person/static object, for the proposed method. More experiments (*e.g.*, the effect of pose quality, the analysis of geometry) can be found on animation in Appendix.

Datasets and Metrics. We leverage three datasets, *i.e.*, BEHAVE [4], ZJU-mocap [45] and CO3D [48] for the compositional human-object neural animation. BEHAVE [4] is a 4D dataset with 8 subjects performing a wide range of interactions with 20 common objects from 4 camera views. BEHAVE provides estimated body poses and object poses for each interaction, while each interaction has less than 50 frames. BEHAVE includes many blurred faces and frames, which we provide the analysis in supplementary materials. ZJU-mocap [45] consists of 10 sequences captured with 23 calibrated cameras. We select one subject (386) and four cameras for evaluating compositional HOI animation on novel persons. CO3D is a large 3D object dataset with multiple sequences. We select "bowl" for evaluation on novel objects. More objects are illustrated in Appendix. We adopt the popular metrics in animatable avatars, peak signal-to-noise ratio (PSNR) and structural similarity index (SSIM).

Table 1: Human-Object Animation under novel interactions. ARAH [59]* indicates we apply the neural human-object deformation to ARAH [59].

Method	backpack		chairblack		chairwood		suitcase		tablesmall		tablesquare		yogaball	
	PNSR	SSIM												
TAVA [28]	27.9	0.960	28.3	0.959	26.0	0.960	28.9	0.964	25.7	0.965	22.8	0.943	24.6	0.950
ARAH [59]	27.9	0.969	28.4	0.970	25.9	0.972	29.3	0.971	25.5	0.976	22.8	0.966	24.9	0.960
ARAH [59]*	27.4	0.971	27.3	0.967	24.6	0.959	28.8	0.978	25.2	0.973	24.7	0.968	27.2	0.976
Baseline	27.8	0.969	28.3	0.969	25.9	0.963	28.8	0.971	26.1	0.967	26.3	0.963	28.2	0.973
CHONA (ours)	28.4	0.971	29.1	0.971	27.3	0.969	29.4	0.974	27.9	0.974	27.9	0.966	28.2	0.974

5.1. Novel Pose Animation

In order to evaluate the novel pose animation, we select the first subject (S01), four kinds of different boxes, and seven classes of objects with distinct interactions from the BEHAVE dataset to construct a benchmark for novel pose animation. The objects with distinct interactions, including “backpack”, “chairwood”, “chairblack”, “suitcase”, “tablesmall”, “tablesquare” and “yogaball” are utilized to evaluate novel actions animation. The boxes consist of four scales, *i.e.*, “boxtiny”, “boxsmall”, “boxmedium” and “boxlarge”, and we leverage it to demonstrate the effectiveness of the proposed method on different scales of objects. We randomly split the training and validation set for boxes, while we randomly choose two or one interaction in other classes for training and the remaining one for validation. The details can be found in supplementary materials. For each interaction in BEHAVE [4], there are only less than 50 frames. Therefore, we use one V100 GPU to run our experiments with 100,000 iterations.

Methods. For a robust comparison, we use template-free model TAVA [28] and model-based method ARAH [59] as our baseline methods. Meanwhile, we apply the neural human-object deformation to ARAH for demonstration and further devise a baseline method with only object localization control. The details of those methods can be found in Appendix.

Quantitative Comparisons. Table 1 illustrates the proposed method considerably improves the baseline Methods among different objects. Without object modelling, TAVA [28] and ARAH [59] fail to render the novel interactions. Particularly, if we apply the neural human-object deformation to the model-based Avatar method (*i.e.*, ARAH [59]), the model can reconstruct the simple object, *e.g.*, “yogaball”, but achieve worse results for the complex objects (*e.g.*, “chairblack”, “chairwood”). We think it is challenging to reconstruct implicit object shapes for ray tracing in ARAH. Table 2 demonstrates that the proposed method consistently improves the baseline methods on boxes, and the larger the box is, the better

Table 2: Human-Object Animation for the boxes, *i.e.*, different sizes of objects.

Method	boxlarge		boxmedium		boxsmall		boxtiny	
	PNSR	SSIM	PNSR	SSIM	PNSR	SSIM	PNSR	SSIM
TAVA [28]	22.6	0.949	25.9	0.967	26.8	0.970	27.5	0.973
ARAH [59]	23.3	0.963	26.3	0.972	27.0	0.974	27.7	0.977
CHONA	27.2	0.971	28.5	0.976	28.0	0.974	28.3	0.976

the performance of the proposed method is. Visualized comparison in Appendix shows the small object, *e.g.*, “boxsmall”, only occupies a small region in the HOI images. Therefore, for those interactions, PNSR and SSIM can not well-demonstrate the model performance.

Qualitative Comparisons. Figure 3 shows our method can effectively animate the human-object interactions under the control of poses. Without the modeling of objects, the baseline methods achieve poor performance on object rendering though it can still render the human body correctly. ARAH with neural human-object deformation (ARAH*) can reconstruct the “yogaball”, but fail to reconstruct the “chairwood”, and even fail to animate the body. We think the self-occlusion of HOI and the failure in reconstructing the complex object cause the model did not achieve a good human-object deformation generalization.

5.2. Compositional Animation

In this subsection, we provide experiments to evaluate the proposed method on the compositional Human-Object Animation. We first construct a compositional benchmark for compositional animation with two subjects (S01, S02) and nine objects, totally 18 combinations, from BEHAVE to construct a sub-dataset. Human-Object Interaction is composed of person, action, and object. There are at most three actions in BEHAVE. Therefore, the subset includes 37 combinations of $\langle \text{person}, \text{action}, \text{object} \rangle$. Given a person, there are different novel compositions as follows,

- Novel Action, *i.e.*, the combination of the object and the person exists in the training set, but the action is

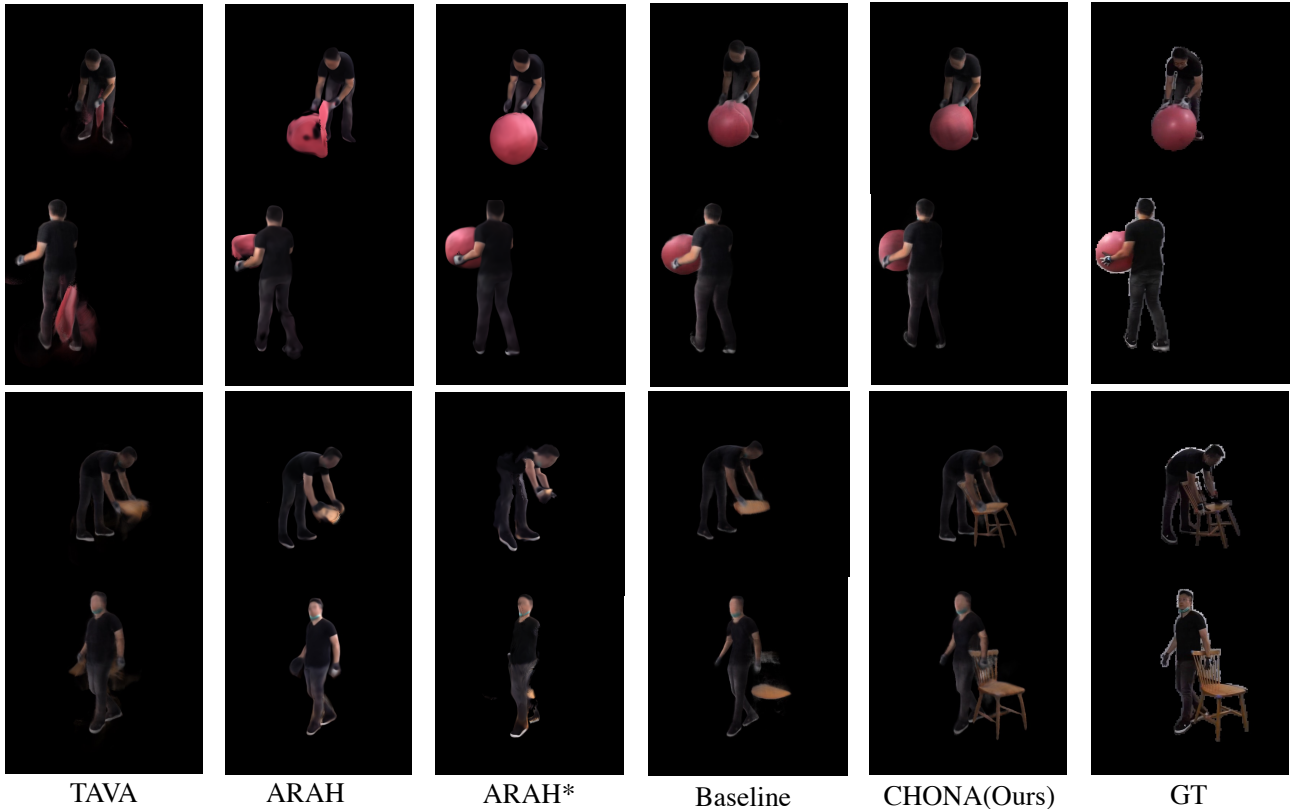


Figure 3: Visualized Comparisons between the proposed method, baseline methods (TAVA [28], ARAH [59]). We demonstrate the results of “yogaball” and “chairwood” with two distinct views. Video demos for better comparison are also provided in the supplementary materials.

novel. This is similar to novel pose animation.

- Novel Object, *i.e.*, there are no combinations of the person and the object in the training set, but the combination of the action and the object exists in the training set.
- Novel Action and Object, *i.e.*, the combination of the action and the object does not exist in the training set.

We then split the dataset into a training set and three validation sets, *i.e.*, novel action validation, novel object validation and novel action-object validation. For similar objects, we treat the actions with the same name equally. For example, the action “sit” between “chairwood” and “chairblack” is treated equally. Then, we randomly select 13 (around 1/3) combinations as the training set, and split the remaining combinations into three novel categories according to the description above. There are 614 frames in the training set, we thus use two V100 GPUs to run our experiments with 300,000 iterations.

Comparisons. The proposed CC-NeRF effectively improves the rendering for both human and object as illus-

Table 3: Compositional Human-Object Animation. The subscripts of a , o and ao indicate the results of novel action set, novel object set, novel action-object set respectively. CIL indicates compositional invariant learning.

Method	PSNR _a	SSIM _a	PSNR _o	SSIM _o	PSNR _{ao}	SSIM _{ao}
w/o CIL	28.2	0.967	26.5	0.961	27.4	0.964
CC-NeRF	28.1	0.966	27.0	0.966	28.0	0.968

trated in Table 3. We notice CC-NeRF achieves similar performance to the network without compositional invariant learning on novel action/pose animation. However, for the novel object split and novel action-object split, The proposed method effectively decomposes the control of different people and objects, and thus illustrates better performance on the compositional animation. Figure 4 demonstrates that the head (the mask is missing) in the baseline is dissimilar to the ground truth, but more similar to another subject. The objects of the baseline become red due to the entangling of the two latent codes. Those cases indicate CC-NeRF effectively decomposes the latent codes and achieves compositional animation.

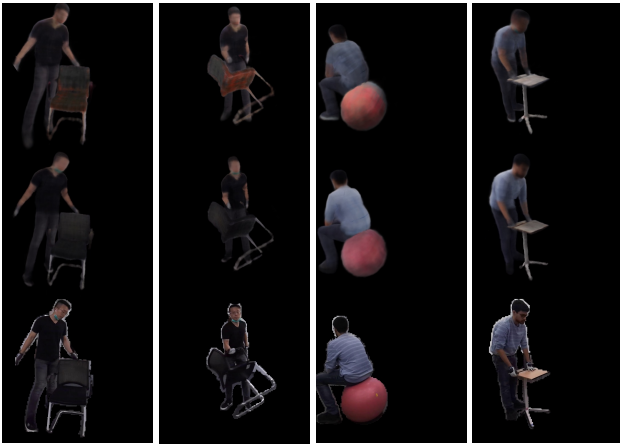


Figure 4: Visual comparisons between the proposed CC-NeRF and the baseline method (w/o CIL). The first row is the baseline, the second row is the proposed method, and the last row is ground truth. The first two columns indicate novel object categories, and the last two columns show novel action-object categories.



Figure 5: Visual comparisons between the proposed CC-NeRF and the baseline (w/o CIL) on novel object and person animation. The first column is novel/object, the second column is the baseline method, the third column is the proposed method, and the last column is the given pose. The first three rows indicate novel person animation, while the last two rows show novel object animation.

5.3. Novel Person and Static Object

The proposed method is not only effective for compositional animation, but also useful for transferring the inter-

Table 4: Comparison on novel static objects (“chairwood”). CIL indicates compositional invariant learning.

Method	PNSR _{ind}	SSIM _{ind}	PNSR _{ood}	SSIM _{ood}
w/o CIL	25.1	0.944	27.1	0.960
CC-NeRF	27.4	0.956	29.2	0.965

actions to non-interactive person and static object, which is more challenging and requires to effectively disentangle the interdependence among person, object and poses. We leverage the person (386) in ZJU-mocap and object bowl in CO3D to jointly train with BEHAVE. Here, for the dataset in BEHAVE, we directly adopt the subset in Section 5.2. We observe the Compositional Conditional NeRF significantly improves the animation for novel object and person as illustrated in Figure 5. We find the method without CIL will incur wired color on the object (*e.g.*, the suitcase) or render the color of the novel person into the object (*e.g.*, the “tablesquare” is green). Besides, for the novel object, we observe the baseline fails to render the human body. More visualized demonstration with additional objects and persons is provided in Appendix. Table 4 further quantitatively show the superior performance on novel static object animation. Here, we select only one frame from “chairwood” and two action sets of “chairblack” for training. We split the validation set into “ind” (similar actions) and “ood” (novel actions). The quantitative comparison for novel person is provided in Appendix.

6. Conclusion and Future Work

In this paper, we address the challenge of compositional human-object animation via neural Human-Object skinning deformations and compositional conditional radiance fields. Specifically, we construct a pseudo bone for the object, and devise a human-object skinning deforming approach to model the interactions between human and object. Moreover, to enable compositional Human-Object animation, we further present compositional conditional neural radiance fields, which decompose the human and object latent codes via compositional invariant learning, to compositionally control the animation for novel human-object combinations, and even novel person and objects. Comprehensive experiments demonstrate the proposed method significantly improves the animation performance, as well as the compositional generalization. Though we achieve considerable performance with the proposed methods, there still are some challenges, *e.g.*, how to understand the interaction region (*i.e.*, affordance region of the object). As human interacts with similar objects in a similar way, we think we can make use of the similarity of affordances among similar objects for the affordance localization to novel objects in the future.

Besides, we devise a compositional animation approach to transfer the interaction poses among similar objects to ease the challenge to capture interaction poses. However, it might be more beneficial to generate the object poses from the human motion poses according to the corresponding interaction categories since there are considerable collected human action poses, which we leave to future work.

References

- [1] Mykhaylo Andriluka and Leonid Sigal. Human context: Modeling human-human interactions for monocular 3d pose estimation. In *International Conference on Articulated Motion and Deformable Objects*, pages 260–272. Springer, 2012. [2](#)
- [2] Dragomir Anguelov, Praveen Srinivasan, Daphne Koller, Sebastian Thrun, Jim Rodgers, and James Davis. Scape: shape completion and animation of people. In *ACM SIGGRAPH 2005 Papers*, pages 408–416. 2005. [4](#)
- [3] Jonathan T. Barron, Ben Mildenhall, Dor Verbin, Pratul P. Srinivasan, and Peter Hedman. Mip-NeRF 360: Unbounded Anti-Aliased Neural Radiance Fields. In *2022 IEEE/CVF Conference on Computer Vision and Pattern Recognition (CVPR)*, pages 5460–5469, New Orleans, LA, USA, June 2022. IEEE. [1, 3, 4](#)
- [4] Bharat Lal Bhatnagar, Xianghui Xie, Ilya A Petrov, Cristian Sminchisescu, Christian Theobalt, and Gerard Pons-Moll. Behave: Dataset and method for tracking human object interactions. In *Proceedings of the IEEE/CVF Conference on Computer Vision and Pattern Recognition*, pages 15935–15946, 2022. [2, 3, 5, 6, 12](#)
- [5] Xu Chen, Yufeng Zheng, Michael J Black, Otmar Hilliges, and Andreas Geiger. Snarf: Differentiable forward skinning for animating non-rigid neural implicit shapes. In *Proceedings of the IEEE/CVF International Conference on Computer Vision*, pages 11594–11604, 2021. [3, 4](#)
- [6] Yixin Chen, Siyuan Huang, Tao Yuan, Siyuan Qi, Yixin Zhu, and Song-Chun Zhu. Holistic++ scene understanding: Single-view 3d holistic scene parsing and human pose estimation with human-object interaction and physical commonsense. In *Proceedings of the IEEE/CVF International Conference on Computer Vision*, pages 8648–8657, 2019. [2](#)
- [7] Zhiqin Chen and Hao Zhang. Learning implicit fields for generative shape modeling. In *Proceedings of the IEEE/CVF Conference on Computer Vision and Pattern Recognition*, pages 5939–5948, 2019. [3](#)
- [8] Rishabh Dabral, Soshi Shimada, Arjun Jain, Christian Theobalt, and Vladislav Golyanik. Gravity-Aware Monocular 3D Human-Object Reconstruction. In *2021 IEEE/CVF International Conference on Computer Vision (ICCV)*, pages 12345–12354, Montreal, QC, Canada, Oct. 2021. IEEE. [2](#)
- [9] Mingsong Dou, Philip Davidson, Sean Ryan Fanello, Sameh Khamis, Adarsh Kowdle, Christoph Rhemann, Vladimir Tankovich, and Shahram Izadi. Motion2fusion: real-time volumetric performance capture. *ACM Transactions on Graphics*, 36(6):1–16, Nov. 2017. [1](#)
- [10] Mingsong Dou, Sameh Khamis, Yury Degtyarev, Philip Davidson, Sean Ryan Fanello, Adarsh Kowdle, Sergio Orts Escolano, Christoph Rhemann, David Kim, Jonathan Taylor, et al. Fusion4d: Real-time performance capture of challenging scenes. *ACM Transactions on Graphics (ToG)*, 35(4):1–13, 2016. [1](#)
- [11] Mihai Fieraru, Mihai Zanfir, Elisabeta Oneata, Alin-Ionut Popa, Vlad Olaru, and Cristian Sminchisescu. Three-dimensional reconstruction of human interactions. In *Proceedings of the IEEE/CVF Conference on Computer Vision and Pattern Recognition*, pages 7214–7223, 2020. [2](#)
- [12] Abhinav Gupta, Aniruddha Kembhavi, and Larry S Davis. Observing human-object interactions: Using spatial and functional compatibility for recognition. *IEEE transactions on pattern analysis and machine intelligence*, 31(10):1775–1789, 2009. [2](#)
- [13] Vladimir Guzov, Aymen Mir, Torsten Sattler, and Gerard Pons-Moll. Human POSEitioning System (HPS): 3D Human Pose Estimation and Self-localization in Large Scenes from Body-Mounted Sensors. In *2021 IEEE/CVF Conference on Computer Vision and Pattern Recognition (CVPR)*, pages 4316–4327, Nashville, TN, USA, June 2021. IEEE. [2](#)
- [14] Sanjay Haresh, Xiaohao Sun, Hanxiao Jiang, Angel X. Chang, and Manolis Savva. Articulated 3D Human-Object Interactions from RGB Videos: An Empirical Analysis of Approaches and Challenges, Sept. 2022. arXiv:2209.05612 [cs]. [2](#)
- [15] Sanjay Haresh, Xiaohao Sun, Hanxiao Jiang, Angel X Chang, and Manolis Savva. Articulated 3d human-object interactions from rgb videos: An empirical analysis of approaches and challenges. *arXiv preprint arXiv:2209.05612*, 2022. [3](#)
- [16] Mohamed Hassan, Duygu Ceylan, Ruben Villegas, Jun Saito, Jimei Yang, Yi Zhou, and Michael J Black. Stochastic scene-aware motion prediction. In *Proceedings of the IEEE/CVF International Conference on Computer Vision*, pages 11374–11384, 2021. [2](#)
- [17] Mohamed Hassan, Partha Ghosh, Joachim Tesch, Dimitrios Tzionas, and Michael J. Black. Populating 3D Scenes by Learning Human-Scene Interaction. In *2021 IEEE/CVF Conference on Computer Vision and Pattern Recognition (CVPR)*, pages 14703–14713, Nashville, TN, USA, June 2021. IEEE. [2](#)
- [18] Mohamed Hassan, Partha Ghosh, Joachim Tesch, Dimitrios Tzionas, and Michael J Black. Populating 3d scenes by learning human-scene interaction. In *Proceedings of the IEEE/CVF Conference on Computer Vision and Pattern Recognition*, pages 14708–14718, 2021. [2](#)
- [19] Zhi Hou, Xiaojiang Peng, Yu Qiao, and Dacheng Tao. Visual compositional learning for human-object interaction detection. In *European Conference on Computer Vision*, pages 584–600. Springer, 2020. [3](#)
- [20] Zhi Hou, Baosheng Yu, Yu Qiao, Xiaojiang Peng, and Dacheng Tao. Affordance transfer learning for human-object interaction detection. In *Proceedings of the IEEE/CVF Conference on Computer Vision and Pattern Recognition*, pages 495–504, 2021. [3](#)
- [21] Yinghao Huang, Omid Taheri, Michael J Black, and Dimitrios Tzionas. Intercap: Joint markerless 3d tracking of hu-

- mans and objects in interaction. In *DAGM German Conference on Pattern Recognition*, pages 281–299. Springer, 2022. [2](#), [3](#)
- [22] Sumit Jain and C. Karen Liu. Interactive synthesis of human-object interaction. In *Proceedings of the 2009 ACM SIGGRAPH/Eurographics Symposium on Computer Animation - SCA '09*, page 47, New Orleans, Louisiana, 2009. ACM Press. [2](#)
- [23] Yuheng Jiang, Suyi Jiang, Guoxing Sun, Zhusu Su, Kaiwen Guo, Minye Wu, Jingyi Yu, and Lan Xu. NeuralHOFusion: Neural Volumetric Rendering under Human-object Interactions. In *2022 IEEE/CVF Conference on Computer Vision and Pattern Recognition (CVPR)*, pages 6145–6155, New Orleans, LA, USA, June 2022. IEEE. [2](#), [3](#)
- [24] Keizo Kato, Yin Li, and Abhinav Gupta. Compositional learning for human object interaction. In *Proceedings of the European Conference on Computer Vision (ECCV)*, pages 234–251, 2018. [3](#)
- [25] Vladimir G Kim, Siddhartha Chaudhuri, Leonidas Guibas, and Thomas Funkhouser. Shape2pose: Human-centric shape analysis. *ACM Transactions on Graphics (TOG)*, 33(4):1–12, 2014. [2](#)
- [26] Diederik P Kingma and Jimmy Ba. Adam: A method for stochastic optimization. *arXiv preprint arXiv:1412.6980*, 2014. [5](#)
- [27] Youngjoong Kwon, Dahun Kim, Duygu Ceylan, and Henry Fuchs. Neural Human Performer: Learning Generalizable Radiance Fields for Human Performance Rendering. In *Advances in Neural Information Processing Systems*, volume 34, pages 24741–24752. Curran Associates, Inc., 2021. [2](#), [3](#)
- [28] Ruilong Li, Julian Tanke, Minh Vo, Michael Zollhofer, Jürgen Gall, Angjoo Kanazawa, and Christoph Lassner. Tava: Template-free animatable volumetric actors. 2022. [2](#), [3](#), [4](#), [5](#), [6](#), [7](#)
- [29] Zhengqi Li, Simon Niklaus, Noah Snavely, and Oliver Wang. Neural Scene Flow Fields for Space-Time View Synthesis of Dynamic Scenes. In *2021 IEEE/CVF Conference on Computer Vision and Pattern Recognition (CVPR)*, pages 6494–6504, Nashville, TN, USA, June 2021. IEEE. [1](#)
- [30] Zongmian Li, Jiri Sedlar, Justin Carpentier, Ivan Laptev, Nicolas Mansard, and Josef Sivic. Estimating 3d motion and forces of person-object interactions from monocular video. In *Proceedings of the IEEE/CVF Conference on Computer Vision and Pattern Recognition*, pages 8640–8649, 2019. [2](#)
- [31] Zhe Li, Zerong Zheng, Hongwen Zhang, Chaonan Ji, and Yebin Liu. Avatarcap: Animatable avatar conditioned monocular human volumetric capture. In *ECCV*, 2022. [3](#)
- [32] Lingjie Liu, Marc Habermann, Viktor Rudnev, Kripasindhu Sarkar, Jiatao Gu, and Christian Theobalt. Neural actor: Neural free-view synthesis of human actors with pose control. *ACM Transactions on Graphics (TOG)*, 40(6):1–16, 2021. [2](#), [3](#)
- [33] Yunze Liu, Yun Liu, Che Jiang, Kangbo Lyu, Weikang Wan, Hao Shen, Boqiang Liang, Zhoujie Fu, He Wang, and Li Yi. Hoi4d: A 4d egocentric dataset for category-level human-object interaction. In *Proceedings of the IEEE/CVF Conference on Computer Vision and Pattern Recognition*, pages 21013–21022, 2022. [2](#)
- [34] Matthew Loper, Naureen Mahmood, Javier Romero, Gerard Pons-Moll, and Michael J Black. Smpl: A skinned multi-person linear model. *ACM transactions on graphics (TOG)*, 34(6):1–16, 2015. [3](#), [4](#)
- [35] Lars Mescheder, Michael Oechsle, Michael Niemeyer, Sebastian Nowozin, and Andreas Geiger. Occupancy networks: Learning 3d reconstruction in function space. In *CVPR*, pages 4460–4470, 2019. [1](#), [3](#)
- [36] Ben Mildenhall, Pratul P Srinivasan, Matthew Tancik, Jonathan T Barron, Ravi Ramamoorthi, and Ren Ng. Nerf: Representing scenes as neural radiance fields for view synthesis. *Communications of the ACM*, 65(1):99–106, 2021. [1](#), [3](#), [4](#), [5](#)
- [37] Megha Nawhal, Mengyao Zhai, Andreas Lehrmann, Leonid Sigal, and Greg Mori. Generating videos of zero-shot compositions of actions and objects. In *European Conference on Computer Vision*, pages 382–401. Springer, 2020. [3](#)
- [38] Michael Niemeyer and Andreas Geiger. Giraffe: Representing scenes as compositional generative neural feature fields. In *Proceedings of the IEEE/CVF Conference on Computer Vision and Pattern Recognition*, pages 11453–11464, 2021. [1](#), [3](#)
- [39] Atsuhiro Noguchi, Xiao Sun, Stephen Lin, and Tatsuya Harada. Neural articulated radiance field. In *Proceedings of the IEEE/CVF International Conference on Computer Vision*, pages 5762–5772, 2021. [2](#), [3](#)
- [40] Ahmed AA Osman, Timo Bolkart, and Michael J Black. Star: Sparse trained articulated human body regressor. In *European Conference on Computer Vision*, pages 598–613. Springer, 2020. [4](#)
- [41] Jeong Joon Park, Peter Florence, Julian Straub, Richard Newcombe, and Steven Lovegrove. Deepsdf: Learning continuous signed distance functions for shape representation. In *Proceedings of the IEEE/CVF conference on computer vision and pattern recognition*, pages 165–174, 2019. [3](#)
- [42] Keunhong Park, Utkarsh Sinha, Jonathan T. Barron, Sofien Bouaziz, Dan B Goldman, Steven M. Seitz, and Ricardo Martin-Brualla. Nerfies: Deformable Neural Radiance Fields. In *2021 IEEE/CVF International Conference on Computer Vision (ICCV)*, pages 5845–5854, Montreal, QC, Canada, Oct. 2021. IEEE. [1](#), [2](#)
- [43] Keunhong Park, Utkarsh Sinha, Peter Hedman, Jonathan T. Barron, Sofien Bouaziz, Dan B Goldman, Ricardo Martin-Brualla, and Steven M. Seitz. Hypernerf: A higher-dimensional representation for topologically varying neural radiance fields. *ACM Trans. Graph.*, 40(6), dec 2021. [1](#), [2](#)
- [44] Sida Peng, Junting Dong, Qianqian Wang, Shangzhan Zhang, Qing Shuai, Xiaowei Zhou, and Hujun Bao. Animatable Neural Radiance Fields for Modeling Dynamic Human Bodies. In *2021 IEEE/CVF International Conference on Computer Vision (ICCV)*, pages 14294–14303, Montreal, QC, Canada, Oct. 2021. IEEE. [2](#), [3](#), [4](#), [5](#)
- [45] Sida Peng, Yuanqing Zhang, Yinghao Xu, Qianqian Wang, Qing Shuai, Hujun Bao, and Xiaowei Zhou. Neural Body: Implicit Neural Representations with Structured Latent Codes for Novel View Synthesis of Dynamic Humans.

- In 2021 IEEE/CVF Conference on Computer Vision and Pattern Recognition (CVPR), pages 9050–9059, Nashville, TN, USA, June 2021. IEEE. 1, 3, 5
- [46] Albert Pumarola, Enric Corona, Gerard Pons-Moll, and Francesc Moreno-Noguer. D-NeRF: Neural Radiance Fields for Dynamic Scenes. In 2021 IEEE/CVF Conference on Computer Vision and Pattern Recognition (CVPR), pages 10313–10322, Nashville, TN, USA, June 2021. IEEE. 1
- [47] Albert Pumarola, Enric Corona, Gerard Pons-Moll, and Francesc Moreno-Noguer. D-nerf: Neural radiance fields for dynamic scenes. In Proceedings of the IEEE/CVF Conference on Computer Vision and Pattern Recognition, pages 10318–10327, 2021. 1
- [48] Jeremy Reizenstein, Roman Shapovalov, Philipp Henzler, Luca Sbordone, Patrick Labatut, and David Novotny. Common objects in 3d: Large-scale learning and evaluation of real-life 3d category reconstruction. In International Conference on Computer Vision, 2021. 5
- [49] Johannes L Schonberger and Jan-Michael Frahm. Structure-from-motion revisited. In CVPR, pages 4104–4113, 2016. 1
- [50] Katja Schwarz, Yiyi Liao, Michael Niemeyer, and Andreas Geiger. Graf: Generative radiance fields for 3d-aware image synthesis. Advances in Neural Information Processing Systems, 33:20154–20166, 2020. 3
- [51] Shih-Yang Su, Timur Bagautdinov, and Helge Rhodin. Danbo: Disentangled articulated neural body representations via graph neural networks. In European Conference on Computer Vision, 2022. 3
- [52] Shih-Yang Su, Frank Yu, Michael Zollhoefer, and Helge Rhodin. A-NeRF: Articulated Neural Radiance Fields for Learning Human Shape, Appearance, and Pose. In Advances in Neural Information Processing Systems, volume 34, pages 12278–12291. Curran Associates, Inc., 2021. 2, 3
- [53] Guoxing Sun, Xin Chen, Yizhang Chen, Anqi Pang, Pei Lin, Yuheng Jiang, Lan Xu, Jingyi Yu, and Jingya Wang. Neural Free-Viewpoint Performance Rendering under Complex Human-object Interactions. In Proceedings of the 29th ACM International Conference on Multimedia, pages 4651–4660, Virtual Event China, Oct. 2021. ACM. 2
- [54] Omid Taheri, Nima Ghorbani, Michael J. Black, and Dimitrios Tzionas. GRAB: A dataset of whole-body human grasping of objects. In European Conference on Computer Vision (ECCV), 2020. 2
- [55] Edgar Treitschke, Ayush Tewari, Vladislav Golyanik, Michael Zollhofer, Christoph Lassner, and Christian Theobalt. Non-Rigid Neural Radiance Fields: Reconstruction and Novel View Synthesis of a Dynamic Scene From Monocular Video. In 2021 IEEE/CVF International Conference on Computer Vision (ICCV), pages 12939–12950, Montreal, QC, Canada, Oct. 2021. IEEE. 1
- [56] Jingbo Wang, Yu Rong, Jingyuan Liu, Sijie Yan, Dahua Lin, and Bo Dai. Towards diverse and natural scene-aware 3d human motion synthesis. In Proceedings of the IEEE/CVF Conference on Computer Vision and Pattern Recognition, pages 20460–20469, 2022. 2
- [57] Jiashun Wang, Huazhe Xu, Jingwei Xu, Sifei Liu, and Xiaolong Wang. Synthesizing long-term 3d human motion and interaction in 3d scenes. In Proceedings of the IEEE/CVF Conference on Computer Vision and Pattern Recognition, pages 9401–9411, 2021. 2
- [58] Shaofei Wang, Marko Mihajlovic, Qianli Ma, Andreas Geiger, and Siyu Tang. MetaAvatar: Learning Animatable Clothed Human Models from Few Depth Images. In Advances in Neural Information Processing Systems, volume 34, pages 2810–2822. Curran Associates, Inc., 2021. 4
- [59] Shaofei Wang, Katja Schwarz, Andreas Geiger, and Siyu Tang. Arah: Animatable volume rendering of articulated human sdbs. In European Conference on Computer Vision, 2022. 2, 3, 4, 5, 6, 7
- [60] Xi Wang, Gen Li, Yen-Ling Kuo, Muhammed Kocabas, Emre Aksan, and Otmar Hilliges. Reconstructing action-conditioned human-object interactions using commonsense knowledge priors. arXiv preprint arXiv:2209.02485, 2022. 2, 3
- [61] Ping Wei, Yibiao Zhao, Nanning Zheng, and Song-Chun Zhu. Modeling 4d human-object interactions for joint event segmentation, recognition, and object localization. IEEE transactions on pattern analysis and machine intelligence, 39(6):1165–1179, 2016. 2
- [62] Chung-Yi Weng, Brian Curless, Pratul P Srinivasan, Jonathan T Barron, and Ira Kemelmacher-Shlizerman. Humannerf: Free-viewpoint rendering of moving people from monocular video. In Proceedings of the IEEE/CVF Conference on Computer Vision and Pattern Recognition, pages 16210–16220, 2022. 3
- [63] Wenqi Xian, Jia-Bin Huang, Johannes Kopf, and Changil Kim. Space-time Neural Irradiance Fields for Free-Viewpoint Video. In 2021 IEEE/CVF Conference on Computer Vision and Pattern Recognition (CVPR), pages 9416–9426, Nashville, TN, USA, June 2021. IEEE. 1
- [64] Xianghui Xie, Bharat Lal Bhatnagar, and Gerard Pons-Moll. Chore: Contact, human and object reconstruction from a single rgb image. In Computer Vision–ECCV 2022: 17th European Conference, Tel Aviv, Israel, October 23–27, 2022, Proceedings, Part II, pages 125–145. Springer, 2022. 2, 3
- [65] Hongyi Xu, Thimo Alldieck, and Cristian Sminchisescu. H-NeRF: Neural Radiance Fields for Rendering and Temporal Reconstruction of Humans in Motion. In Advances in Neural Information Processing Systems, volume 34, pages 14955–14966. Curran Associates, Inc., 2021. 2
- [66] Xiang Xu, Hanbyul Joo, Greg Mori, and Manolis Savva. D3d-hoi: Dynamic 3d human-object interactions from videos. arXiv preprint arXiv:2108.08420, 2021. 2
- [67] Bangbang Yang, Yinda Zhang, Yinghao Xu, Yijin Li, Han Zhou, Hujun Bao, Guofeng Zhang, and Zhaopeng Cui. Learning object-compositional neural radiance field for editable scene rendering. In Proceedings of the IEEE/CVF International Conference on Computer Vision (ICCV), pages 13779–13788, October 2021. 1, 3
- [68] Jason Y. Zhang, Sam Pepose, Hanbyul Joo, Deva Ramanan, Jitendra Malik, and Angjoo Kanazawa. Perceiving 3d human-object spatial arrangements from a single image in the wild. In European Conference on Computer Vision (ECCV), 2020. 2

- [69] Siwei Zhang, Yan Zhang, Qianli Ma, Michael J Black, and Siyu Tang. Place: Proximity learning of articulation and contact in 3d environments. In *2020 International Conference on 3D Vision (3DV)*, pages 642–651. IEEE, 2020. [2](#)
- [70] Xiaohan Zhang, Bharat Lal Bhatnagar, Sebastian Starke, Vladimir Guzov, and Gerard Pons-Moll. Couch: towards controllable human-chair interactions. In *Computer Vision–ECCV 2022: 17th European Conference, Tel Aviv, Israel, October 23–27, 2022, Proceedings, Part V*, pages 518–535. Springer, 2022. [3](#)
- [71] Yan Zhang, Mohamed Hassan, Heiko Neumann, Michael J Black, and Siyu Tang. Generating 3d people in scenes without people. In *Proceedings of the IEEE/CVF conference on computer vision and pattern recognition*, pages 6194–6204, 2020. [2](#)
- [72] Fuqiang Zhao, Wei Yang, Jiakai Zhang, Pei Lin, Yingliang Zhang, Jingyi Yu, and Lan Xu. Humannerf: Efficiently generated human radiance field from sparse inputs. In *Proceedings of the IEEE/CVF Conference on Computer Vision and Pattern Recognition*, pages 7743–7753, 2022. [3](#)
- [73] Kaifeng Zhao, Shaofei Wang, Yan Zhang, Thabo Beeler, and Siyu Tang. Compositional Human-Scene Interaction Synthesis with Semantic Control, July 2022. arXiv:2207.12824 [cs]. [2](#)
- [74] Kaifeng Zhao, Shaofei Wang, Yan Zhang, Thabo Beeler, and Siyu Tang. Compositional human-scene interaction synthesis with semantic control. *arXiv preprint arXiv:2207.12824*, 2022. [2, 3](#)
- [75] Zerong Zheng, Han Huang, Tao Yu, Hongwen Zhang, Yandong Guo, and Yebin Liu. Structured Local Radiance Fields for Human Avatar Modeling. In *2022 IEEE/CVF Conference on Computer Vision and Pattern Recognition (CVPR)*, pages 15872–15882, New Orleans, LA, USA, June 2022. IEEE. [2, 3, 5](#)
- [76] Keyang Zhou, Bharat Lal Bhatnagar, Jan Eric Lenssen, and Gerard Pons-Moll. Toch: Spatio-temporal object-to-hand correspondence for motion refinement. In *Computer Vision–ECCV 2022: 17th European Conference, Tel Aviv, Israel, October 23–27, 2022, Proceedings, Part III*, pages 1–19. Springer, 2022. [3](#)

A. Benchmark Construction

In our experiment, we randomly choose one action as validation set for each subject-object pair to evaluate the performance on out-of-distribution poses.

Here we provide the interactions splits of our experiments in Table 5. For boxes, we randomly split the frames into training set and validation set because there is only a single interaction for each box. For compositional animation, we select “yogaball”, “chair-black”, “chairwood”, “tablesquare”, “tablesmall”, “suitcase”, “boxmedium”, “boxlarge”, “boxsmall” from BEHAVE [4] to construct the benchmark. Table 6 present the splits of compositional animation.

B. Challenges Analysis on BEHAVE

Occlusions BEHAVE [4] is a real-world 3D HOI dataset with *only four camera views and extensive occlusions*, which poses a significant challenge for the detailed reconstruction of Human and Object. Meanwhile, each interaction has less than 50 frames, which is challenging for the model to implicitly reconstruct the human body and object.

Blurry faces and frames To protect privacy, BEHAVE [4] uses the mask or fuzzy technique to blur most of the faces as illustrated in Figure 6. This makes it very difficult to reconstruct the face of Subject01. Meanwhile, there are also blurry frames in BEHAVE. This further poses a significant challenge for a detailed reconstruction of HOI as illustrated in Figure 6.

Inaccurate Segmentation Besides, the segmentation mask in BEHAVE [4] is not much accurate due to the occlusion and complex background as illustrated in Figure 7. One can find more inaccurate segmentation in the ground truth of the video comparison. In our experiment, we find the proposed method is able to marginally implicitly reconstruct the object and human body. However, the segmentation problem also degrades the accuracy of reconstruction.

Table 5: Dataset splits for novel pose animation.

Objects	training set	validation set
backpack	Date01_Sub01_backpack_hug, Date01_Sub01_backpack_back	Date01_Sub01_backpack_hand
chairwood	Date01_Sub01_chairwood_hand, Date01_Sub01_chairwood_sit	Date01_Sub01_chairwood_lift
chairblack	Date01_Sub01_chairblack_lift, Date01_Sub01_chairblack_hand	Date01_Sub01_chairblack_sit
suitcase	Date01_Sub01_suitcase_lift	Date01_Sub01_suitcase
tablesmall	Date01_Sub01_tablesmall_lift, Date01_Sub01_tablesmall_move	Date01_Sub01_tablesmall_lean
tablesquare	Date01_Sub01_tablesquare_hand, Date01_Sub01_tablesquare_lift	Date01_Sub01_tablesquare_sit
yogaball	Date01_Sub01_yogaball	Date01_Sub01_yogaball_play

Table 6: Dataset splits for compositional animation.

training set	novel action validation	novel object validation	novel action object validation
Sub01_chairwood_hand, Sub01_chairwood_lift, Sub01_tablesmall_lean, Sub01_tablesmall_lift, Sub01_yogaball_play, Sub02_boxmedium_hand, Sub02_boxsmall_hand, Sub02_chairblack_hand, Sub02_chairblack_lift, Sub02_suitcase_ground, Sub02_tablesquare_sit, Sub02_tablesquare_lift, Sub01_boxlarge_hand	Sub01_yogaball, Sub02_suitcase_lift, Sub01_chairwood_sit, Sub02_chairblack_sit, Sub01_tablesmall_move, Sub02_tablesquare_move, Sub01_suitcase	Sub01_chairblack_sit, Sub02_chairwood_sit, Sub01_suitcase_lift, Sub02_yogaball_sit, Sub02_tablesmall_move, Sub01_tablesquare_hand	Sub01_chairblack_hand, Sub01_chairblack_lift, Sub02_chairwood_hand, Sub02_yogaball_play, Sub02_tablesmall_lean, Sub02_tablesmall_lift, Sub01_tablesquare_sit, Sub01_tablesquare_lift, Sub02_boxlarge_hand, Sub01_boxmedium_hand, Sub01_boxsmall_hand

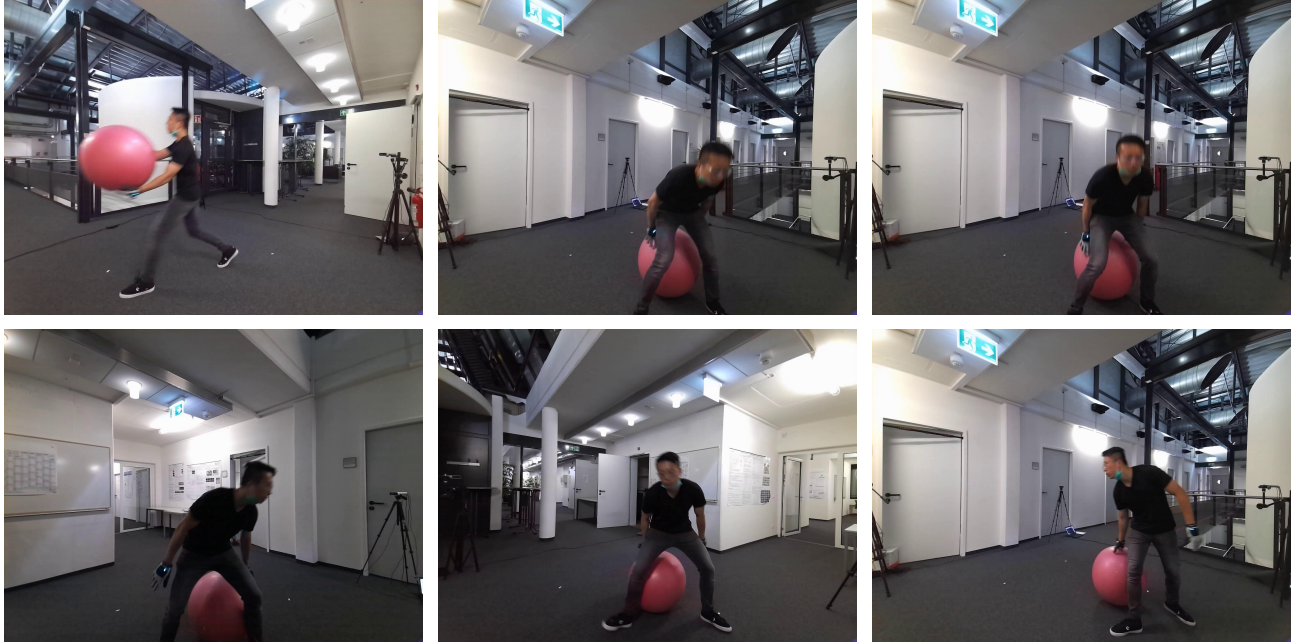


Figure 6: Illustration of the blurry faces and frames.

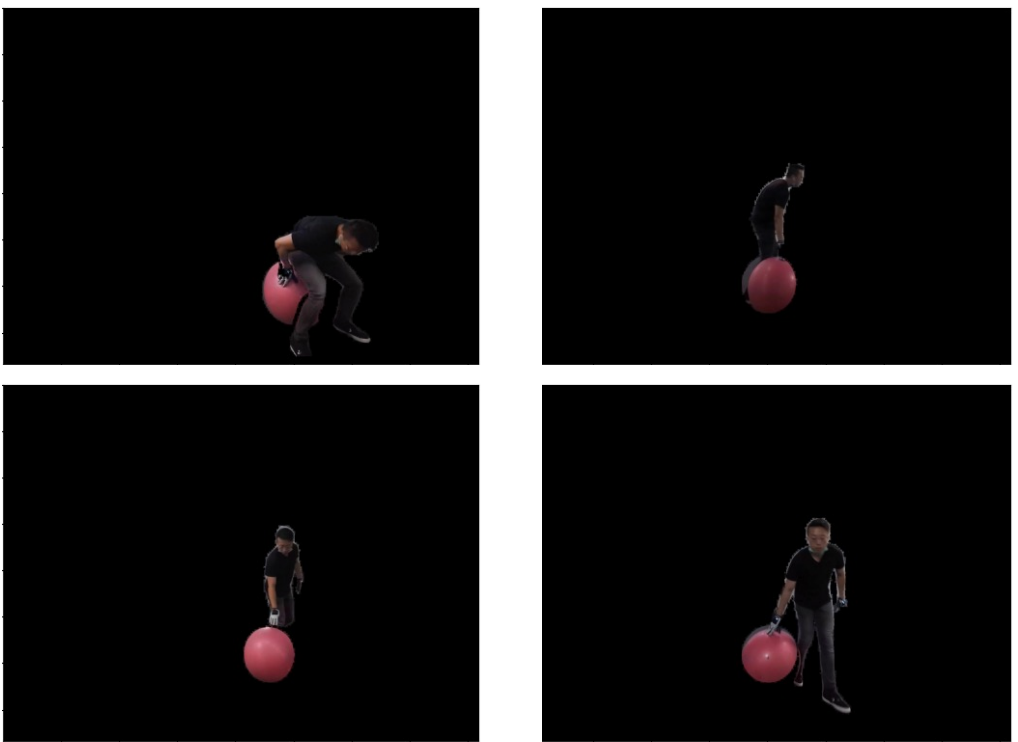


Figure 7: Illustration of inaccurate masks. The boundary between the yogaball and human is not correct. The wrong boundary even causes the shape of yogaball changes.